THE ASTROPHYSICAL JOURNAL, 422:L59–L62, 1994 February 20

BATSE OBSERVATIONS OF THE VERY INTENSE GAMMA-RAY BURST GRB 930131

CHRYSSA KOUVELIOTOU[1]
Universities Space Research Association
ROBERT PREECE,[2] NARAYANA BHAT,[3] GERALD J. FISHMAN, CHARLES A. MEEGAN, AND JOHN M. HORACK
NASA/Marshall Space Flight Center, Huntsville, AL 35812
MICHAEL S. BRIGGS, WILLIAM S. PACIESAS, AND GEOFFREY N. PENDLETON
Department of Physics, University of Alabama in Huntsville, Huntsville, AL 35899
DAVID BAND AND JIM MATTESON
CASS 0111, University of California, San Diego, La Jolla, CA 92093
AND
DAVID PALMER,[2] BONNARD TEEGARDEN, AND JAY P. NORRIS
NASA/Goddard Space Flight Center, Greenbelt, MD 20771
Received 1993 June 22; accepted 1993 December 2

ABSTRACT

BATSE observed its most intense gamma-ray burst on 1993 January 31. The event reached count rates $\gtrsim 2 \times 10^6$ counts s^{-1} with most of the flux emitted in an extremely short ($\lesssim 0.1$ s) interval followed by a long tail, lasting about 50 s. Most of this initial pulse was recorded by our instrument with unique, very high temporal resolution (1 ms). We were thus able to show large changes in spectral hardness on 2 ms timescales throughout this initial complex. Photons as low as 25 keV and extending up to >4 MeV in energy were recorded by BATSE during this first interval. The burst spectrum is best fitted by a broken power law with a break energy of 170 ± 27 keV. The low-energy spectral index is -1.30 ± 0.05, while a softer spectral index of -1.9 fits the spectrum between 170 keV and 2 MeV. Our data provide the only low-energy spectrum for this event; the combination of our spectrum with the one reported for GRB 930131 by the EGRET group extends the total energy spectrum of a GRB for the first time over five decades, up to the GeV range.

Subject heading: gamma-rays: bursts

1. INTRODUCTION

On 1993 January 31 at 18:57 UT, the Burst and Transient Source Experiment (BATSE) (Fishman et al. 1989) onboard the Compton Gamma-Ray Observatory (CGRO), triggered on the most intense event of the over 600 gamma-ray bursts (GRBs) it detected during its first 2 years of operation. We present here the only high-resolution time history and energy spectrum between 25 and 1900 keV for this event. Three companion *Letters* give additional information on the high-energy part of the spectrum of the event as recorded with the Energetic Gamma Ray Experiment Telescope (EGRET) (Sommer et al. 1994), preliminary results on its direction of arrival from the Compton Telescope (COMPTEL) (Ryan et al. 1994), and results of multiwavelength searches for counterparts of the source (Schaefer et al. 1994).

2. GRB 930131 DATA CHARACTERISTICS

BATSE has eight large-area detectors (LADs), optimized for high trigger sensitivity and time resolution, and eight spectroscopy detectors (SDs), optimized for high-energy resolution. At all times the experiment transmits several data types from all detectors. On 1993 January 31, the instrument triggered at 68231.682 s UT; this was the end of the first 64 ms time interval in which the second brightest LAD count rates exceeded the background level by 5.5 σ. All times cited hereafter are relative to the trigger time of 68231.682 s UT. The start time of the high energy resolution LAD and SD (HERB/SHERB) data types (see Table 1) is delayed relative to the trigger time (for GRB 930131) by a maximum of 0.064 s. No pretrigger time-tagged events data are available: TTE data begin at 0.010 s and STTE data begin at 0.008 s.

The onboard computer ranks the LAD detectors by brightness at trigger time; data from the four brightest detectors are accumulated for the burst data types (Table 1). During the first 64 ms of GRB 930131, the burst flux incident upon the source-facing LADs was consistent with count rates of a few MHz. Over this time interval, the LADs suffered extreme deadtime, pulse pile-up, and other electronic effects, too severe to be utilized; the SDs, however, are smaller and less severely affected, so that their data can be reliably corrected throughout the entire burst. The Earth-facing LADs received a large flux scattered by the terrestrial atmosphere which, while large, did not overload these detectors. This effect, combined with the severe electronic effects mentioned above, resulted in the source-facing detectors recording fewer counts than the Earth-facing LADs; they were thus ranked by the onboard computer as being lower in brightness. As a consequence, the highest time resolution spectra available for GRB 930131 were collected from the Earth-facing LADs and therefore not used; the usable spectra for GRB 930131 were accumulated from the source-facing detectors with lower time resolution. Table 2 lists

[1] Postal address: NASA/Marshall Space Flight Center, Huntsville, AL 35812.
[2] NRC/NAS Resident Research Associate.
[3] NRC/NAS Senior Research Associate; on leave from Tata Institute of Fundamental Research, Bombay 400 005, India.

TABLE 1

DATA TYPES AND TIME COVERAGE FOR GRB 930131

Data Type	Full Name	Type[a]	Energy Channels	Time Resolution	Time Coverage
LAD Disc	Discriminator	B/T	4	64 ms	Always
LAD CONT	Continuous	B/T	16	2.048 s	Always
LAD HERB	High-Energy Resolution Burst	T	128	≥512 ms	0.064:23.9 s
LAD TTE	Time-Tagged Events	T	4	2 μs	0.010:0.085 s
SD Disc	Discriminator	B/T	4	2.048 s	Always
SHERB	SD High-Energy Resolution Burst	T	256	≥512 ms	0.064:122.4 s
STTE	SD Time-Tagged Events	T	256	128 μs	0.008:1.52 s

[a] B: background data, T: trigger data types.

the characteristics of the burst-selected detectors for GRB 930131.

3. TEMPORAL ANALYSIS

Figure 1 progressively resolves the temporal structure of GRB 930131. In Figure 1*a*, we plot the LAD rates above 25 keV, recorded with 1.024 s time resolution. The burst profile is truncated to exhibit best the tail of the event, which lasts until approximately 50 s after the trigger. The dotted line on the plot represents a quadratic fit to the background. The initial main complex of pulses ($t \approx -0.05$ to 1.4 s), recorded with 0.064 s time resolution, splits into two subpulses (Fig. 1*b*). We note that the last 64 ms bin prior to the burst trigger time does not represent the true burst counting rate at the peak. We have used the SD data to estimate what the true LAD counting rate was, as we discuss later.

Figure 1*c* depicts the burst profile using TTE data accumulated into three energy ranges. The rates are corrected for deadtime; pulse pile-up effects were negligible for this data type. The data start at 0.010 s and last for ~0.075 s; they are plotted with 1 ms time resolution. The low-energy profile is relatively smooth, while at high energy it resolves into a finer structure of at least two subpulses. Figure 1*d* shows the second main peak of Figure 1*b* with a time resolution of 8 ms using STTE data. We show data from two SDs (4 and 5), which are not set at the same gain and therefore have different energy ranges. The solid line corresponds to the sum of rates for both detectors below 300 keV, while the dotted line shows the sum above 300 keV. No additional structure is seen at higher energies for this pulse, even at higher time resolution.

TABLE 2

DETECTOR DESCRIPTION

On-Board Rank	Detector	SD Burst Angle	SD Earth Angle	Energy Range (keV)	LAD Burst Angle	LAD Earth Angle
1.....	3	133.7	44.6	300–21000	152.5	25.8
2.....	1	105.0	73.2	25–2500	121.3	57.3
3.....	4	46.3	135.4	300–21000	27.5	154.2
4.....	5	79.4	102.3	15–1450	98.0	83.7

NOTES.—All angles are in degrees. The source and Earth angles are measured from the detector normal to the vector to the burst and Earth's center, respectively. The SD energy range is the energy range of the SHER/SHERB high resolution data; the SD discriminators cover a wider range. For the LADs, the high-resolution data spans ≈25 to >1900 keV.

Figure 2 shows the rates of the source-facing SD 5 in two discriminator energy channels at 2.048 s time resolution. There is highly significant flux above 4 MeV in one interval, which ends at $t = 0.128$ s, thereby encompassing all of the initial

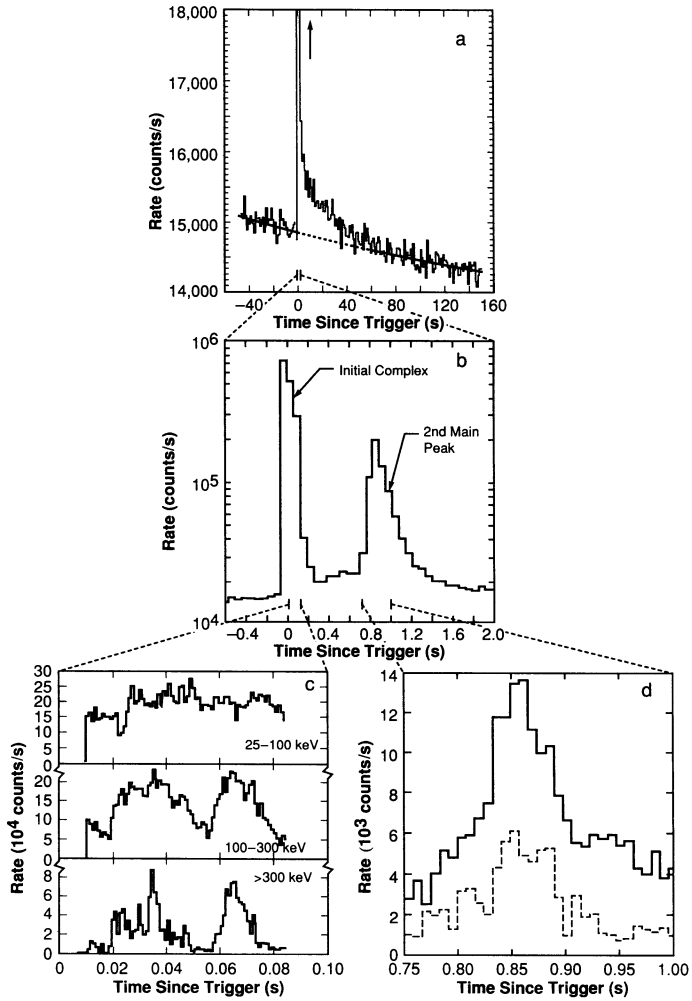

FIG. 1.—Time history of GRB 930131. (*a*) Total burst profile above 25 keV integrated with 1.024 s time resolution. The plot is truncated (as indicated by the upward arrow) to emphasize the weaker part (tail) of the event. The dotted line shows the background fit. (*b*) Expansion of the first 2 s of the event as indicated on (*a*). The time resolution is 0.064 ms. (*c*) TTE data integrated in three energy ranges with 1 ms time resolution, corresponding to the decaying part of the initial complex (as indicated). (*d*) STTE data in two energy ranges plotted with 8 ms time resolution.

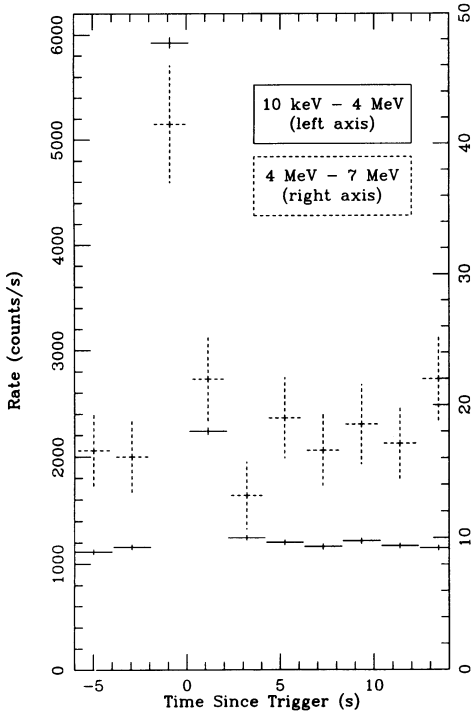

FIG. 2.—Count rates from SPEC detector 5 in two discriminator channels (*solid and dotted lines*) plotted with 2.048 s time resolution.

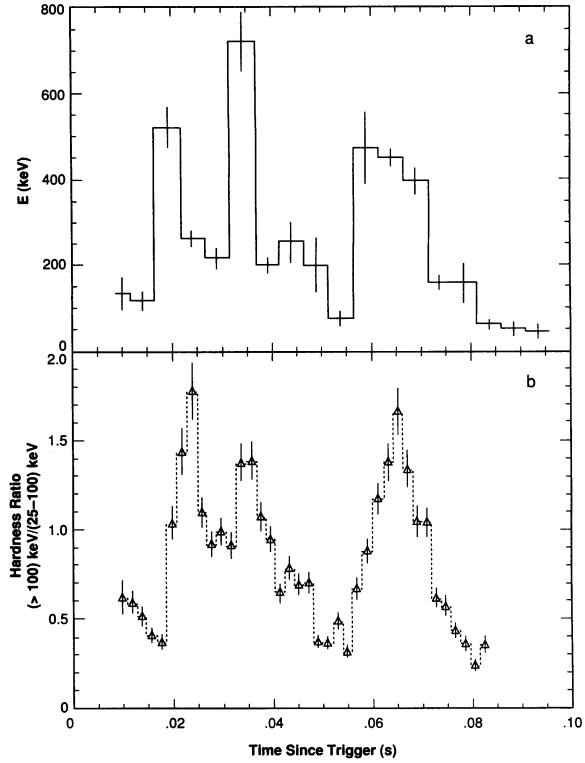

FIG. 3.—Spectral evolution of the initial complex (Fig. 1*b*). (*a*) Peak energy of the vF_v spectrum from SDs 4 and 5, plotted with 5 ms time resolution. (*b*) Hardness ratios in 2 ms steps of the same complex from LAD 4.

complex (Fig. 1*b*). When we normalize the LAD rates to the SD rates, we find that the "true" LAD peak rate for the first 0.1 s summed over the four selected detectors is $\gtrsim 2 \times 10^6$ counts s^{-1}! This extreme count rate explains the severe dead-time effects experienced by all (except for the SDs) *CGRO* instruments (Sommer et al. 1994; Ryan et al. 1994). Using the SD discriminator data, the fluence of the first high-rate 2.048 s interval, integrated between 100 and 1000 keV, is found to be a few $\times 10^{-5}$ ergs cm^{-2}. The fluence of the next 50 s, calculated using the LAD CONT data between 25 and 1900 keV, is an order of magnitude lower, i.e. a few $\times 10^{-6}$ ergs cm^{-2}, consistent with the numbers reported by EGRET (Sommer et al. 1994).

4. SPECTRAL ANALYSIS

4.1. *Spectroscopy Detector Data*

We fit the STTE background-subtracted spectra from two detectors (SD 4 and 5), with a model in which a low-energy power law (spectral index α) with an exponential cutoff (cutoff energy E_0) connects smoothly with a high-energy power law (spectral index β) (Band et al. 1993). The fits and the photon spectra based on them show that the curvature, measured by the difference of the power law indices α and β, was greater for the initial emission complex (Fig. 1*b*) than for the second main peak. The low-energy power-law indices range from ≈ -0.9 to 0.1; however, the exact values are highly correlated with the fitted values for E_0. To minimize the errors at the high-energy part of the spectrum, we rebinned the STTE data from $t = 0.008$ to 1.275 s into eight broad channels: we find 3 σ detections in the channels up to 1500 keV, and a 2 σ detection in the 5000–10000 keV channel. In general, the spectrum from the first complex is flatter (harder) at low energy, and steeper (softer) at high energy. Note that the STTE data do not cover the beginning (first peak at $t < 0.01$ s) of the initial emission complex which may have been much harder than the remainder of this complex. This assumption is corroborated by the SD discriminator data of Figure 2, which clearly show that there was highly significant flux above 4 MeV before the start of the high-resolution data.

Figure 3*a* shows the evolution in time (in 5 ms bins) of the energy of the peak $[E = (2 + \alpha)E_0]$ in the vF_v spectrum of each feature of the initial complex. The spectra were binned into 16 nearly logarithmic channels. Figure 3*b* shows the hardness ratios (the ratios of the counts above 100 keV and between 25 and 100 keV) of the TTE data for the decaying part of the initial complex, in 2 ms bins. Both data sets describe independent measures of the hardness evolution during the event and are in qualitative agreement within the different bin size limitations. This agreement also provides indirect evidence that there are no pulse pile-up effects in the TTE data. We notice large changes in spectral hardness on 2 ms timescales throughout the initial burst complex.

4.2. *Large Area Detector Data*

The LADs have ~ 16 times larger collecting area than do the SDs, and thus they have better counting statistics across their entire energy span. We were able to include the effects of Earth scattering for the LAD analysis, which contributes to a better determination of our response at the low energy end of the spectrum. Usable LAD data are only available after the burst trigger and only for detector 4 (Table 2). The first HERB accumulation ($t = 0.064$: 2.112), covers the decay part of the initial complex and the second main peak. When we fit this

spectrum with the model previously described, we find $\alpha = -1.25 \pm 0.03$, $\beta = -2.5 \pm 0.4$, and $E_0 = 650 \pm 80$ (with χ^2 of 158 for 109 degrees of freedom). The energy of the peak of νF_ν for this spectrum is 490 keV.

A broken power-law fit to the CONT spectrum from $t = 0.099$ to 49.25 s, which covers the second main emission peak and the tail of the burst, yields a break energy of $E = 170 \pm 27$ keV and a spectral index above the break of -1.9 ± 0.1 (with $\chi^2 = 6.6$ for 10 dof). The lower energy power-law index is harder, -1.30 ± 0.05, corroborating the spectral curvature discussed in the previous section. As Figure 1*a* shows, there is considerable emission in a gradually decaying tail lasting ≈ 50 s. To search for spectral evolution in the tail, we binned together the CONT data from $t = 2.14$ to 49.2 s into 6 time bins, between 25 and 1900 keV. Each time interval was then fit to a broken power-law model keeping the break energy fixed at 170 keV. The weighted means of the lower/higher energy indices are -1.2 ± 0.1 and -1.9 ± 0.1, respectively.

5. DISCUSSION

We have detected an extremely intense GRB which had the highest count rates recorded so far with BATSE. We present here the time history of this event with temporal resolution and sensitivity that is unique among all observations of GRB 930131. We detect weak emission for ~ 50 s after the ~ 0.1 s initial peak. Our results establish the long duration of GRB 930131 and confirm that the EGRET detection of GeV photons several seconds after the peak (Sommer et al. 1994) is not discrepant and could indeed be related to the burst. We have detected emission of high-energy photons with $E \gtrsim 4$ MeV during the initial peak. The fact that we do not see an excess of 4 MeV photons during the tail of the event in our data does not exclude their presence at the same relative level throughout the burst.

BATSE provides the only spectrum that extends to lower energies ($\gtrsim 25$ keV) for GRB 930131. The combined spectrum of the initial peak and the tail exhibits a spectral break around 170 keV; the high-energy part of the spectrum (up to 2000 keV) can be fitted with a single power law with a spectral index of -1.9. Our results are consistent (above 200 keV) with the values reported by COMPTEL (Ryan et al. 1994) and EGRET (Sommer et al. 1994) in both the TASC and spark chamber data for similar time accumulations and energy ranges. We present, for the first time, significant evidence for spectral evolution on 2 ms timescales. Our results demonstrate that future spectral investigations of GRBs must search at the shortest timescales possible in order to probe the spectral signature of the actual emission mechanism at the source, rather than average over an evolving spectrum.

Although GRB 930131 was the most intense event detected with BATSE so far, neither its fluence nor its spectrum are exceptional. Should the presence of very high energy photons in GRBs relate to their fluences, we would expect GeV photons to be detected in many more events with similar fluences and spectra. If, on the other hand, such photons are not detected, one could infer that their presence is related to the peak intensity of an event, rather than its fluence.

We wish to thank J. van Paradijs for several fruitful discussions.

REFERENCES

Band, D., et al. 1993, ApJ, 413, 281
Fishman, G. J., et al. 1989, in Proc. of the GRO Science Workshop, ed. W. N. Johnson (NASA/GSFC), 39
Ryan, J., et al. 1994, ApJ, 422, L67
Schaefer, B., et al. 1994, ApJ, 422, L71
Sommer, M., et al. 1994, ApJ, 422, L63